

OBSERVATIONS ON SUBMICROPULSE ELECTRON-BEAM EFFECTS FROM SHORT-RANGE WAKEFIELDS IN TESLA-TYPE SUPERCONDUCTING RF CAVITIES*

A. H. Lumpkin[#], R. Thurman-Keup, D. Edstrom Jr., P. Prieto, J. Ruan
Fermi National Accelerator Laboratory, Batavia, IL 60510 USA
F. Zhou, J. Diaz-Cruz¹, A. Eleden, B. Jacobson
SLAC National Accelerator Laboratory, Menlo Park, CA 94025 USA
¹also at University of New Mexico, Albuquerque, NM 87131 USA

Abstract

Experiments were performed at The Fermilab Accelerator Science and Technology (FAST) facility to elucidate the effects of short-range wakefields (SRWs) in TESLA-type rf cavities. FAST has a unique configuration of a photocathode rf gun beam injecting two TESLA-type single cavities (CC1 and CC2) in series prior to the cryomodule. To investigate short-range wakefield effects, we have steered the beam to minimize the signals in the higher-order mode (HOM) detectors of CC1 and CC2 for a baseline, and then selected a vertical corrector to steer the beam off axis at an angle into CC1 or CC2. A Hamamatsu synchroscan streak camera viewing a downstream OTR screen provided an image of y-t effects within the micropulses with ~10-micron spatial resolution and 2-ps temporal resolution. At 500 pC/b, 50 b, and 2 mrad off-axis steering into CC2, we observed an ~100-micron head-tail centroid shift in the streak camera image y(t)-profiles. This centroid shift value is consistent with a calculated short-range wakefield effect using ASTRA simulations.

INTRODUCTION

The preservation of the low emittance of electron beams during transport through the accelerating structures of large facilities is an ongoing challenge. In the cases of the TESLA-type superconducting rf cavities currently used in the European X-ray Free-electron Laser (FEL) [1] and the currently-under-construction Linac Coherent Light Source upgrade (LCLS-II XFEL) [2], off-axis beam transport may result in emittance dilution due to transverse long-range (LRW) and short-range wakefields (SRW) [3-5]. To investigate such effects, experiments were performed at the Fermilab Accelerator Science and Technology (FAST) facility with its unique two-cavity configuration after the photocathode rf gun [6]. We used optical transition radiation (OTR) imaging with a UV-visible synchroscan streak camera to display sub-micropulse y-t effects in the 20- and 41-MeV beam.

We report effects on beam transverse position centroids and sizes correlated with off-axis beam steering in TESLA-type cavities. We used a 3-MHz micropulse repetition rate and targeted diagnostics for these tests. Our initial data

from an OTR imaging source indicated our streak camera can provide ~10-micron spatial resolution with 1-2 ps (σ) temporal resolution depending on the bandpass filter employed. Since the observed bunch lengths were 10-20 ps (σ), we had sufficient resolution for up to 20 time slices in the 4σ profile. In this sense we also obtained slice-emittance information (with β -function information). We used the higher-order mode (HOM) detectors and rf BPMs to establish first the desired off-axis steering and then evaluated the short-range wakefield effects on the beam dynamics.

EXPERIMENTAL ASPECTS

The IOTA Electron Injector Linac

The Integrable Optics Test Accelerator (IOTA) electron injector at the FAST facility (Fig. 1) begins with an L-band rf photoinjector gun built around a Cs2Te photocathode (PC). When the UV component of the drive laser, described elsewhere [7] is incident on the PC, the resulting electron bunch train with 3-MHz micropulse repetition rate exits the gun at <5 MeV. Following a short transport section with a pair of trim dipole magnet packages (H/V100 and H/V101), the beam passes through two superconducting rf (SCRf) capture cavities denoted CC1 and CC2, and then a transport section to the low-energy electron spectrometer, D122. Diagnostics used in these studies include the rf BPMs, the imaging screens at X107, X108, X121, and X124, and HOM couplers at the upstream and downstream ends of each SCRf cavity. The HOM signals were processed by the HOM detector circuits with the Schottky diode output provided online through ACNET, the Fermilab accelerator controls network [4]. The HOM detectors' bandpass filters were optimized for two dipole passbands from 1.6 to 1.9 GHz, and the 1.3-GHz fundamental was reduced with a notch filter. The rf BPMs' electronics were configured for bunch-by-bunch capability with optimized system attenuation. At 2 nC per micropulse, the rms noise was found to be 25 μ m in the horizontal axis (x) and 15 μ m in the vertical axis (y) at B101 in the test with 4.5-MeV beam from the gun. However, for these studies on short-range transverse wakefields, we relied on a streak camera to provide the sub-micropulse spatial information.

The Streak Camera System

We utilized a C5680 Hamamatsu streak camera with an S20 PC operating with the M5675 synchroscan vertica

*This manuscript has been authored by Fermi Research Alliance, LLC under Contract No. DE-AC02-07CH11359 with the U.S. Department of Energy, Office of Science, Office of High Energy Physics.
#lumpkin@fnal.gov

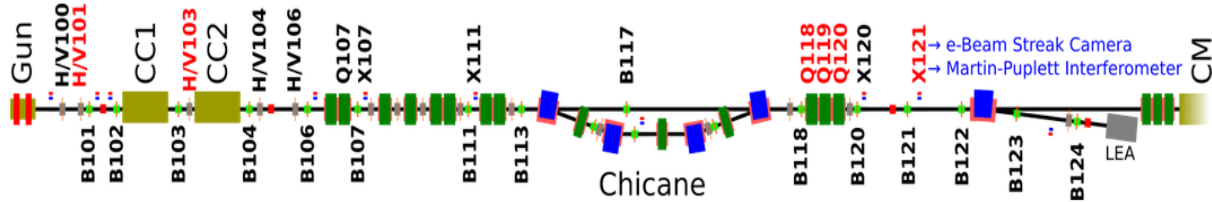


Figure 1: Schematic of the FAST beamline layout showing the PC rf gun, capture cavities (CCn), correctors (H/Vnnn), rf BPMs (Bnnn), chicane, OTR and YAG:Ce screens (Xnnn), the spectrometer dipole bend magnet (D122), and the beginning of the cryomodule (CM).

deflection unit that was phase locked to 81.25 MHz as shown in Fig. 2. In addition, we used a phase-locked-loop C6878 delay box that stabilizes the streak image positions to about 1 ps temporal jitter over 10s of minutes. These steps enabled the synchronous summing of 50-150 micro-pulses or bunches (b) generated at 3 MHz by the photoinjector or the offline summing of 10-100 images to improve statistics in the sum images. We applied the principle to optical transition radiation (OTR) generated from an Al-coated Si substrate at the X121 screen location (see Fig. 1) with subsequent transport to the beamline streak camera. Commissioning of the streak camera system was facilitated through a suite of controls centered around ACNET. This suite includes operational drivers to control and monitor the streak camera as well as Synoptic displays to facilitate interface with the driver. Images were captured from the streak camera using the readout camera, Prosilica 1.3-Mpixel CCD camera with 2/3" format, and were analyzed both online and with an offline MATLAB-based ImageTool processing program [8]. Bunch-length measurements using these techniques have been reported previously from the A0 Facility [9] and FAST first system streak camera commissioning at 20 MeV [10].

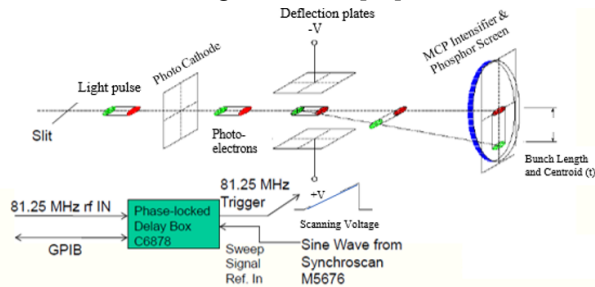


Figure 2: Schematic of the C5680 synchroscan streak camera with phase locking at 81.25 MHz.

EXPERIMENTAL RESULTS

Initial Streak Camera Data:

In order to investigate the short-range, wakefield-driven submicropulse effects, we used the HOM detector signals as a measure of how far off axis the beam was in the cavities. We minimized the HOMs in CC1 and CC2 as the reference point, and then stepped the V103 corrector magnet current values. For the 20-MeV post-CC1 beam energy, a change of 1 A in corrector current corresponded to an ~2-mrad angular steering change into CC2. The transport

optics rotated the image 90° so we observed the vertical spatial information on the horizontal display axis in the streak image from X121. The changes in y-t streak images are shown in Fig. 3 for V103 corrector values 0.0 and -1.0 A compared to the reference. Beam size dilution of 38% was measured at 569 μm as compared to the 413-μm value at 0.0-A setting in the projected profiles. In Fig. 3b, the head-tail kick direction followed the corrector steering polarity, and $\delta y_c = -111 \mu\text{m}$ was observed for one cavity.

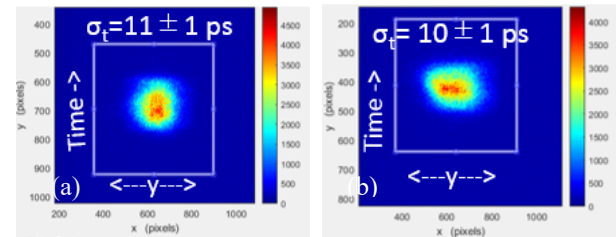


Figure 3: Streak camera images at X121 with V103 = (a) 0.0 and (b) -1.0 A corrector values. The corrector current change of 1 A corresponds to an ~2-mrad angular steering change into CC2.

Space-Charge-Driven Bunch Elongation Effects

The streak images when projected to the time axis provide the electron bunch profile and length. With an initial laser pulse length of 4 ps, we observed the significant electron bunch elongation due to space-charge forces as seen in Fig. 4. In this case the laser spot size was ~ 0.45 mm by 0.56 mm so at 250 pC/b and above the space-charge forces dominated the distributions. In these cases, the final energy was 41 MeV.

Bunch by Bunch rf BPM Data

We also evaluated the potential long-range wakefield or HOM effects on the beam centroid by using the rf BPM data. An example of the centroid motion *within* the 50-micropulse train of a macropulse is shown in Fig. 5 with both noise-reduction and bunch-by-bunch capabilities implemented. The ~220-kHz oscillation seen in the B117 data is a combination of difference frequencies between HOM modes 7 and 14 in CC2 and a beam harmonic [11]. The field oscillations kicked different micropulses according to the amplitude at that point in time, resulting in the sub-macropulse effects. The quadrupole triplet Q118-120 was used to focus the beam smaller horizontally while leaving the vertical size at ~ 1000 μm at the X121 YAG:Ce station.

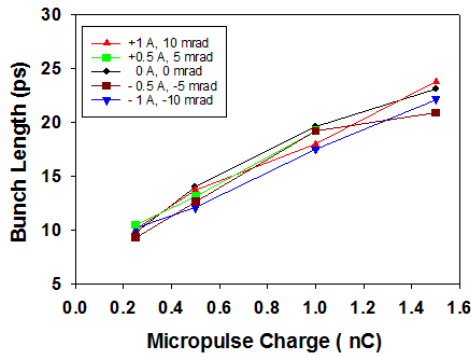


Figure 4: Streak camera bunch length versus charge results during a V101 corrector scan from -1.0- to +1.0-A values. At 4.5 MeV, a 1-A current change corresponds to a 10-mrad angular change into CC1. The transverse laser spot is ~ 0.5 mm in x and y in this case [12].

The beam centroid oscillation amplitude is much reduced to <40 μm at B121 downstream of this triplet, and thus the main competing mechanism identified does not account for all of the observed y-t effect in the streak image. Since the ASTRA simulations for the FAST setup indicated a 500- μm head-tail kick for 500 pC/b and a 5-mm offset at 41 MeV, we attribute the 100- μm head-tail effects for a 2-3 mm offset seen in Fig. 3 to such short-range wakefields.

ASTRA Simulations of the Short-range Wakefield

The ASTRA simulations [13] used the nominal FAST linac input deck with the laser bunch length of 4 ps sigma, a laser transverse spot size of 0.6 mm in x and y, an injection phase of 45° , a gun gradient of 45 MV/m, and the capture cavity gradients of 21 and 14 MV/m for CC1 and CC2, respectively. In particular, the program utilizes the 3D fields of the TESLA-type cavities to produce realistic simulations of the beam through the cavities for comparison to the observations. The simulations were for a single micropulse with 500 pC of charge transiting the two cavities with 0 mm and 5 mm offsets as shown in Fig. 6. The simulation shows a tear-drop shape in y-t space. (envision later time upward) as reported previously [5] and an ~ 500 - μm head-tail kick for the 5-mm offset in Fig. 6b.

In Fig. 7a the elongation of the electron bunch is calculated as $\sigma_t = 13$ ps compared to the 4-ps laser pulse. This is attributed to space-charge forces acting before acceleration in CC1. The charge dependence of the bunch length from ASTRA is shown in Fig. 7b for the laser transverse spot size of 0.6 mm. The electron beam bunch length varies from ~ 10 to 21 ps for 0.25 to 1.5 nC/b, respectively. The similar increase in this bunch length for a slightly smaller laser spot size of 0.5 mm is seen in the direct comparison to the Fig. 4 data.

SUMMARY

In summary, observations of short-range wakefield effects on beam dynamics were made using the streak camera

to obtain y-t images at the submicropulse time scale. The HOM detectors and rf BPMs were used to evaluate off-axis steering related to these tests, and the HOM-induced sub-micropulse centroid motion was shown to be smaller than the observed effects. Moreover, the head-tail centroid kicks were consistent with short-range wakefield results from ASTRA for the TESLA-type superconducting rf cavity and attributed to that effect.

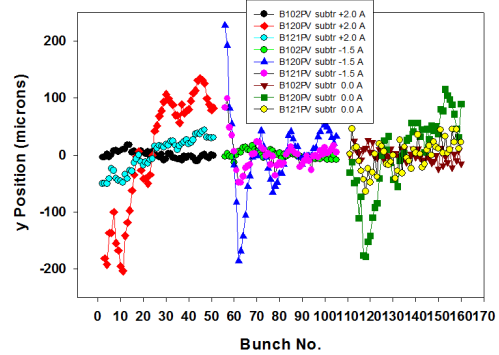


Figure 5: Examples of the variation of the beam vertical centroids bunch by bunch for 50 m icropulses at B102, B120, and B121 for V103 settings of +2.0, -1.5, and 0.0 A from the reference. These were 100-shot averages to show the ~ 220 -kHz oscillation effects generated in CC2 [11].

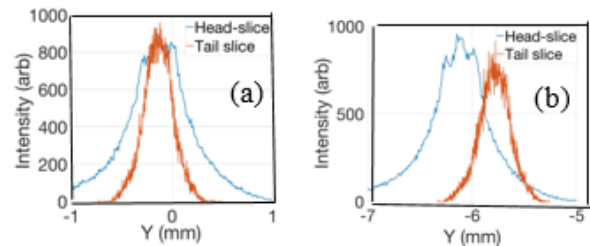


Figure 6: ASTRA simulation results of the head-tail kick for (a) no y offset with no y-t kick and (b) 5-mm y offset through the cavities with a calculated ~ 500 - μm head-tail kick.

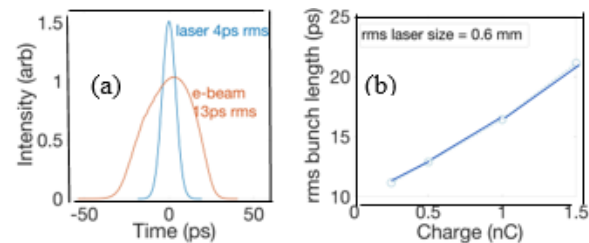


Figure 7: ASTRA simulation results for the electron-beam bunch length at (a) 500 pC/b compared to the initial laser pulse length and (b) as a function of charge from 0.25 to 1.5 nC.

ACKNOWLEDGMENTS

The Fermilab authors acknowledge the support of C. Drennan, A. Valishev, D. Broemmelsiek, G. Stancari, and M. Lindgren, all in the Accelerator Division at Fermilab. The SLAC/NAL authors acknowledge the support of J. Schmerge (Superconducting Linac Division, SLAC).

REFERENCES

- [1] H. Weise and W. Decking, “Commissioning and First Lasing of the European XFEL”, in *Proc. 38th Int. Free Electron Laser Conf. (FEL'17)*, Santa Fe, NM, USA, Aug. 2017, pp. 9-13. doi:10.18429/JACoW-FEL2017-MOC03.
- [2] P. Emma, “Status of the LCLS-II FEL Project at SLAC”, in *Proc. 38th Int. Free Electron Laser Conf. (FEL'17)*, Santa Fe, NM, USA, Aug. 2017, Talk, JACoW-FEL2017-MOD01
- [3] J. T. Seeman *et al.*, “Transverse Wakefield Control and Feedback in the SLC Linac”, in *Proc. 12th Particle Accelerator Conf. (PAC'87)*, Washington D.C., USA, Mar. 1987, pp. 1349-1353.
- [4] A. H. Lumpkin *et al.*, “Submacropulse electron-beam dynamics correlated with higher-order modes in Tesla-type superconducting rf cavities”, *Phys. Rev. Accel. Beams*, vol. 21, no. 6, p. 064401, Jun. 2018. doi:10.1103/physrevaccelbeams.21.064401
- [5] A. H. Lumpkin, R. M. Thurman-Keup, D. Edstrom, and J. Ruan, “Submicropulse electron-beam dynamics correlated with short-range wakefields in Tesla-type superconducting rf cavities”, *Phys. Rev. Accel. Beams*, vol. 23, no. 5, p. 054401, May 2020. doi:10.1103/physrevaccelbeams.23.054401
- [6] M. Church *et al.*, “The ASTA User Facility Proposal”, Fermi National Accelerator Laboratory, Batavia, IL, Rep. Fermilab-TM-2568, Oct. 2013.
- [7] J. Ruan, M. D. Church, D. R. Edstrom, T. R. Johnson, and J. K. Santucci, “Commissioning of the Drive Laser System for Advanced Superconducting Test Accelerator”, in *Proc. 4th Int. Particle Accelerator Conf. (IPAC'13)*, Shanghai, China, May 2013, paper WEPME057, pp. 3061-3063.
- [8] R. Thurman-Keup, FNAL, off-line MATLAB-based Image-Tool Program, 2011.
- [9] A. H. Lumpkin, J. Ruan, and R. Thurman-Keup, “Synchroscan streak camera imaging at a 15-MeV photoinjector with emittance exchange” *Nucl. Instr. and Meth. A* vol. 687, pp. 92-100, Sep. 2012. doi:10.1016/j.nima.2012.05.068
- [10] A. H. Lumpkin, D. R. Edstrom, J. Ruan, J. K. Santucci, and R. M. Thurman-Keup, “Initial Observations of Micropulse Elongation of Electron Beams in a SCRF Accelerator”, in *Proc. North American Particle Accelerator Conf. (NAPAC'16)*, Chicago, IL, USA, Oct. 2016, pp. 337-340. doi:10.18429/JACoW-NAPAC2016-TUPOA26.
- [11] A. H. Lumpkin *et al.*, “Observations of Long-range Wakefield Effects Generated in an Off-Resonance Tesla-Type-Cavity”, presented at IPAC'21, Campinas, Brazil, paper TUPAB272, this conference.
- [12] A. H. Lumpkin, D. R. Edstrom, J. Ruan, R. M. Thurman-Keup, and B. T. Jacobson, “Direct Observations of Submicropulse Electron-Beam Effects from Short-range Wakefields in TESLA-Type Superconducting RF Cavities”, presented at the 9th Int. Beam Instrumentation Conf. (IBIC'20), Santos, Brazil, Sep. 2020, paper TUPP17.
- [13] ASTRA Manual, <https://www.desy.de/~mypf1o/>